

STRIP CROWN AND EDGE DROP SENSITIVITY ANALYSIS OF A 6-HIGH ROLLING MILL

Renan Bueno Wojciechowski

Yukio Shigaki

CEFET-MG, Belo Horizonte, Minas Gerais, Brazil

renanbuenow@gmail.com, yukio.shigaki@cefetmg.br

Abstract. Metal strips with tight tolerances and low cost are highly demanded by customers worldwide. Its production relies on a deep understanding of how operational parameters affect the whole process, in order to develop a robust control strategy. The present work aims to assess how strip's crown and edge drop are affected by intermediate roll shifts, roll bending loads and work roll radius variation for an industrial 6-high cold rolling mill through a sensitivity analysis. The strip exit thickness profile and the contact pressure between work and intermediate rolls are shown, as well. The 3D FEM/Multi-slab method, a hybrid computer model validated with industrial data, is used. This models the rolls of any type with few simplifications and, by running faster than the full finite element model, it is more suitable for a sensitivity analysis. The results show good linear correlation between the strip's crown ($R^2 \approx 99\%$) and edge drop ($R^2 \approx 94\%$) with the roll shift and roll bending force, respectively. On the other hand, the roll radius variation's average R^2 was only 72%, though the range of crown and edge drop values was very small (around 4 to 5 μm). The rolls' contact pressure field shows some peaks that should be considered for premature wear. All 27 cases were simulated in only 2,5 hours.

Keywords: Sensitivity analysis, Strip crown, Edge drop, Finite Element Method

1. INTRODUCTION

Customers worldwide demand the production of steel strips with tight tolerances and less cost from the modern steel industry, more and more. Surface finishing, mechanical properties and strip geometry are some important characteristics to be targeted. Regarding strip geometry, its crown, edge drop and flatness are crucial properties demanded from automotive and electrical sectors, household appliances, food packaging, etc.

Strip crown is a geometrical variable that shows the thickness difference from center to the edge, and its variation in a stand may cause non-flatness problems. Edge drop is a rapid drop at the strip edge, and its control is useful for reducing edge cracks and are very demanded, for example, for electrical steel sheets (Wang Q., et. al, 2018), where a very squared edge improves energy efficiency.

It is recognized that these high quality products can only be achieved from a deep understanding of the rolling process, in order to better control the strip shape, and one way to develop this knowledge is through mathematical and computational modeling.

A model of the rolling mill is a good one when it is validated with industrial data. Once it is done, a sensitivity analysis of the process can be made, with the main purpose of identifying the influence of changing only one parameter over the strip crown and edge drop, for instance. Roll bending force, intermediate roll shift value, diameter of the rolls, strip thicknesses, rear and forward tension, friction coefficient, strip width, etc... are some of the influencing parameters that can be considered. Mill trials to accomplish this analysis require a considerable amount of effort, being almost unfeasible to run keeping all the others parameters fixed (Ginzburg and Azzam, 1997).

The main results from a sensitivity analysis are the development of simple rules that allows us to better understand the rolling mill process and, consequently, achieve a better control and a high quality steel strip.

A common drawback normally arises when a sensitivity analysis is performed with simulators. When these models are complex, e.g., a mill modeled with Finite Element Method (FEM) for both rolls and the strip, each case takes several hours to finish, so that running a dozen or more cases become very tedious. It must be noted that many simplified models for roll stack deformation are limited for simpler rolling mills.

Many authors present sensitivity analysis.

Ginzburg, et al. (2006) presented a rolling mill analysis for many different mills, using FEM for the rolls and considering the strip a series of springs. They introduce the rate effect idea, and this allowed to show more concise graphics of the sensitivity analysis addressed, relating to different strip widths.

Wang Q., et al. (2018) and Wang X., et al. (2020) used an explicit Finite Element simulation of a 6-high stand to obtain a more in-depth knowledge of the effects caused by the intermediate roll shift. The first related it to the exit strip

thickness profile, rolling load, equipment stiffness and stresses due to rolls contact. The second showed that the results obtained for the edge drop could be directly applied on the production line in order to increase the product quality.

Aljabri, *et al.* (2013) made a different approach, studying the influence of roll crossing through extensive field tests that demanded the modification a preexistent rolling mill.

Linghu, *et al.* (2014) used the explicit Finite Element Method to evaluate the strip for 27 distinct cases, which took about 1400 hours of computational running time. Wang X., *et al.* (2020) corroborated with the choice of the method showing that, if executed in a quasi-static way (implicit), it would be even slower. The sensitivity analysis developed by Wang Q., *et al.* (2018) included only 17 cases.

One way to work around this limitation is the use of simplified methods that make the computer simulation faster, but many of them fail for more complex rolling mills, as is the case of a 6-high, with or without CVC rolls. Shigaki, *et al.* (2017) and Shigaki, *et al.* (2019) showed that the study of the strip crown variation due the intermediate roll shift can be easily executed by the hybrid model used in this paper, taking around 9 minutes for each case.

In the present work, a sensitivity analysis of a 6-high rolling mill modeled with a 3D FEM/Multi-slab method is addressed (Fig. 1). In order to better discuss the answers, only the following three parameters will be selected to vary: work roll (WR) bending load, intermediate roll (IMR) shift and WR diameter. The first two are actuator devices commonly used to control the process, especially strip crown and edge drop, and are used together in more than 550 HC-MILL stands worldwide (Kajiwara, *et al.*, 2015). The last one is a parameter that varies continuously along a campaign due to wear, and aims to assess its effect over strip crown and edge drop. Additionally, the normal contact pressures between WR and IMR are shown, as they may lead to high stress peaks, causing damage to the rolls.

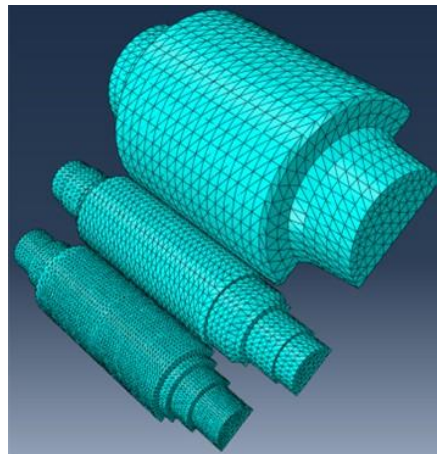


Figure 1. Roll stack finite element mesh

1.1 Influence rolling parameters

1.1.1 Roll bending loads

The roll bending system consists on the application of a vertical load (F) on the roll neck, as shown in Fig. 2. They change the deflection of the rolls, affecting strip crown (Ginzburg, *et al.*, 2009). They can be applied on the WR, IMR and backup (BUR) roll necks, as well.

1.1.2 Intermediate roll shifting

Originally, the IMR was developed to reduce edge drop by reducing the WR deflection by positioning one of its edges right above (or bottom side) the strip edge, which eliminates the unwanted contact between these two rolls (Kajiwara, *et al.*, 2015). This is done by IMR translation along the Y axis of Fig. 2 and allows a certain control of the force flow inside the equipment. This parameter variation range depends on the equipment's specification and is presented in Fig. 2 as δ , the horizontal distance between the edges of intermediate roll and strip.

1.1.3 Work roll diameters

The reduction of the work roll radius (R) along a campaign affects the process in two distinct ways: it changes the roll's deformation and the total rolling load. The first results in more deformation on the equipment, leading to a higher crown, while the second causes the opposite effect (lower radius, lower rolling load). Both effects must be considered in order to define the final strip.

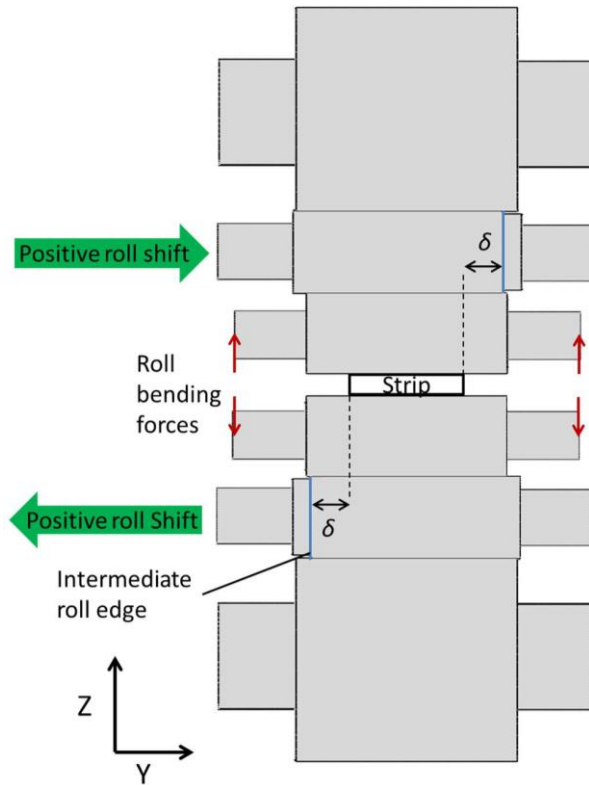


Figure 2. 6-high rolling mill sketch

1.2 Output variables

1.2.1 Strip crown

The strip crown (C) can be defined as in Eq. (1):

$$C = h_c - \frac{h'_j + h''_j}{2} \quad (1)$$

Where the variables (shown in Fig.3) are the thicknesses measured at the center (h_c) and from a predefined distance j from each edge (h'_j and h''_j). Usually j assumes a value of 25 mm or 40 mm.

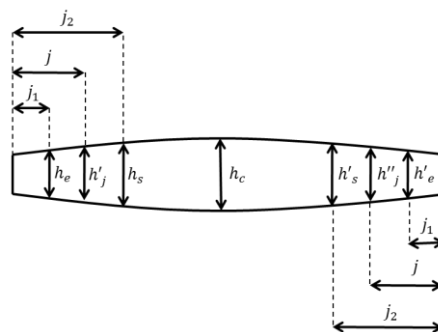


Figure 3. Strip's cross sectional profile.

1.2.2 Edge drop

The edge drop (E_{40}) is calculated through Eq. (2):

$$E_{40} = \frac{(h_s - h_e) + (h'_s - h'_e)}{2} \quad (2)$$

The thickness measurements define how abrupt it varies very near the edges. As shown in Fig.3, these values are called h_e and h_e' when extracted from a distance j_1 of both edges and h_s and h_s' when is j_2 away. It is desirable that a product possesses E_{40} closer to zero (Ginzburg and Azzam, 1997; Wang Q., *et al.*, 2017).

1.2.3 Normal contact pressure between WR and IMR

The WR-IMR contact pressure is calculated along the central line rested on the XY symmetry plane shown on Fig. 2. Despite being, in fact, distributed in an area, pressures along the roll barrel length are normally higher on this central line due the geometrical and load symmetry consideration.

2. DEVELOPMENT

2.1 6-high rolling mill

The equipment to be tested in this study is a 6-high cold rolling mill, similar to that presented by Shigaki, *et al.* (2017). This choice was made because it has been previously validated with industrial data. The main parameters are shown in Tab. 1.

Table 1. Rolling parameters for the previously validated case

Parameter	Value
Mean entry strip thickness (mm)	2,2
Expected exit strip thickness (mm)	1,34
Strip width (mm)	980
Work roll radius (mm)	225
Intermediate roll radius (mm)	210
Backup roll radius (mm)	600
Strain hardening, Y (MPa)	$Y = 230 * 500 * \epsilon^{0,5}$
Front applied tension (MPa)	200
Back applied tension (MPa)	20
Roll bending load (kN)	109
Pivot length (mm)	390
Total measured load (kN)	9000
δ (mm)	50
Friction coefficient	0,0675

2.2 Methods and procedures

The equipment is simulated through the hybrid model (Shigaki, *et al.*, 2017; Shigaki, *et al.*, 2019) with all the parameters of Tab. 1, and one of the following variables is changed: IMR shift (δ), work roll radius (R) and work roll bending force (F). Their values can be seen in Tab. 2.

For the outputs, the strip crown and edge drop are calculated through Eqs. (1) and (2), with predefined distances in Tab. 3. Some of the results of exit thickness profile and the WR-IMR contact pressure are also presented for specific cases.

Table 2. Influence parameters values used in the sensitivity analysis (the interval between the analyzed values for each parameter is constant)

Parameter	Initial value	Final value	Number of tested values
IMR displacement, δ (mm)	0	100	11
Work roll radius, R (mm)	195	225	7
Roll bending force, F (kN)	41,4	414	10

Table 3. Predefined distances utilized on the strip's crown and edge drop calculations

Position of thickness measurement	Value (mm)
j	25,4
j_1	7,5
j_2	40

2.3 Results

The main output values are shown in Tab. 4. Influence parameters and the strip's crown and edge drop are presented in Figs. 4, 6 and 8. For these three figures the exit thickness profile for some specific points are shown in Figs. 5, 7 and 9 and the linear adjustments, in Tab. 5. All the 27 cases were ran in 2,5 hours in a computer with Intel core I7-8700@3,20 GHz processor and 16 GB of RAM.

The variation of δ within the specified range shows that it affects significantly the strip crown, allowing it to have values between 18 μm until 61 μm and edge drop from 30 μm to 37 μm . The same result is possible with the roll bending load, with values of 57 μm until -22 μm for strip crown and 35 μm to 22 μm for edge drop. The variation of work roll radius showed small ranges between 42 μm and 37 μm for the strip's crown and 34 μm and 28 μm for the edge drop, which resulted on the two almost identical thickness profiles shown in Fig. 7. In all the cases, both values are directly proportional to each other.

Based on the original condition, the roll bending is the actuator that, if individually changed, would lead to the flattest strip. If the roll bending force is set to 248,4 kN, it will produce a strip crown of 11 μm and an edge drop of 29 μm . Those values are superior when compared to the test where $\delta = 0$ mm in which they are 18 μm and 31 μm respectively.

Table 4. Main output values of each simulation case (roll shift δ , WR radius R and roll bending force F)

Case	Modified parameter	Parameter value	Crown (μm)	Edge drop (μm)	Maximum value of contact pressure (MPa)	Position X of max contact pressure occurrence (mm)
1	δ	0 mm	18	31	1639	429
2	δ	10 mm	24	30	1921	448
3	δ	20 mm	28	31	1474	448
4	δ	30 mm	33	30	1800	468
5	δ	40 mm	38	32	1559	-565
6	δ	50 mm	42	33	1658	487
7	δ	60 mm	46	34	1181	487
8	δ	70 mm	50	34	1497	507
9	δ	80 mm	54	36	1584	-565
10	δ	90 mm	57	35	1353	526
11	δ	100 mm	61	37	934	526
12	R	195 mm	38	29	1455	487
13	R	200 mm	37	31	1482	487
14	R	205 mm	39	31	1513	487
15	R	210 mm	38	33	1545	487
16	R	215 mm	39	32	1591	487
17	R	220 mm	41	34	1623	487
18	F	41,4 kN	57	35	1580	487
19	F	82,8 kN	47	35	1631	487
20	F	124,2 kN	39	32	1682	487
21	F	165,6 kN	29	31	1738	487
22	F	207 kN	20	29	1786	487
23	F	248,4 kN	11	29	1839	487
24	F	289,8 kN	2	26	1901	487
25	F	331,2 kN	-6	24	1970	487
26	F	372,6 kN	-15	23	2028	487
27	F	414 kN	-22	22	2095	487

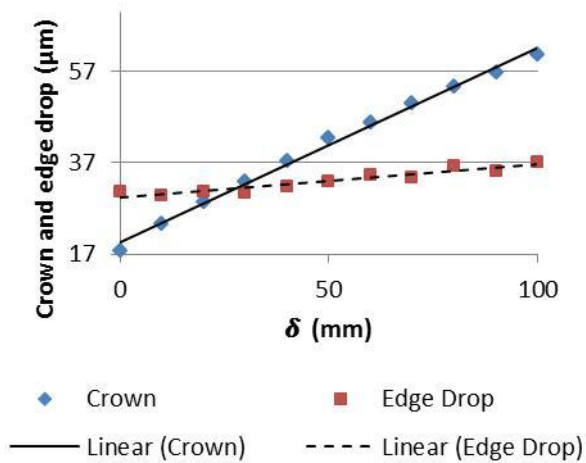


Figure 4. Strip's crown and edge drop due to roll shift (δ) variation.

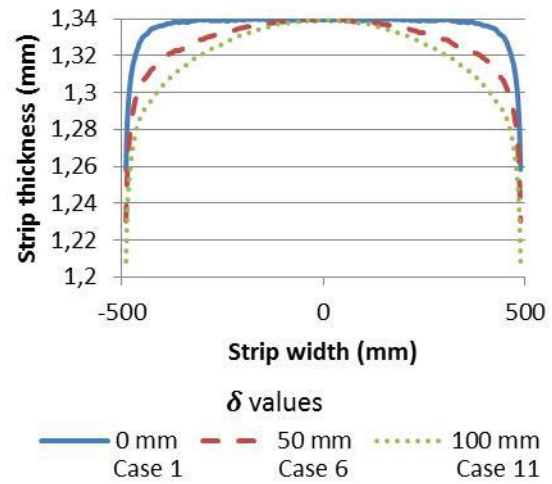


Figure 5. Exit strip thickness profile for δ values

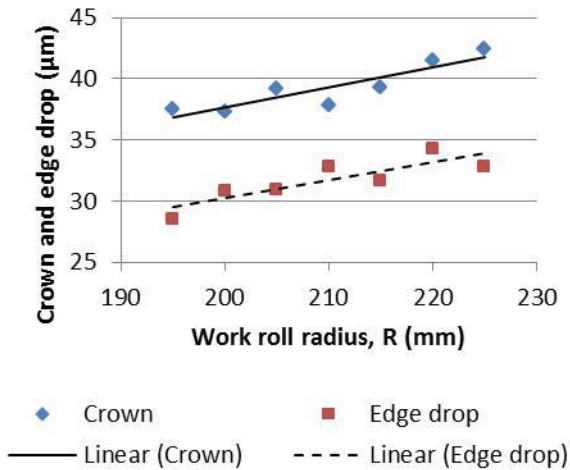


Figure 6. Strip's crown and edge drop due to work roll radius variation

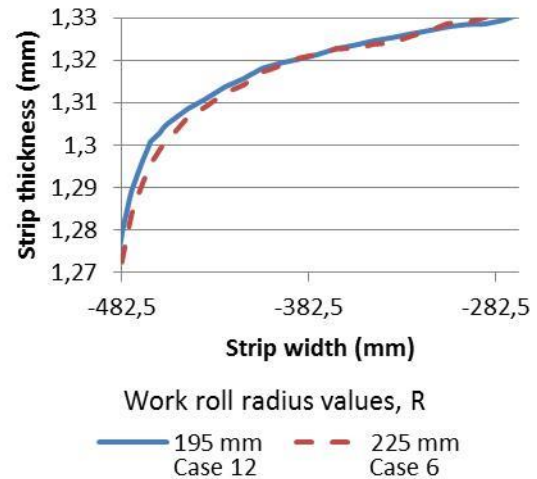


Figure 7. Part of the exit strip thickness profile obtained with two values of work roll radius

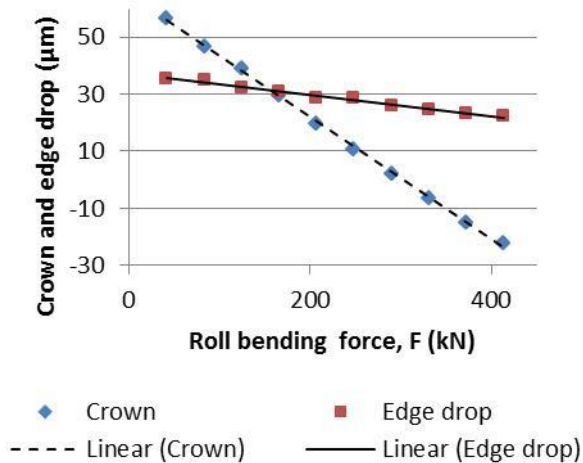


Figure 8. Strip's crown and edge drop due to roll bending force variation

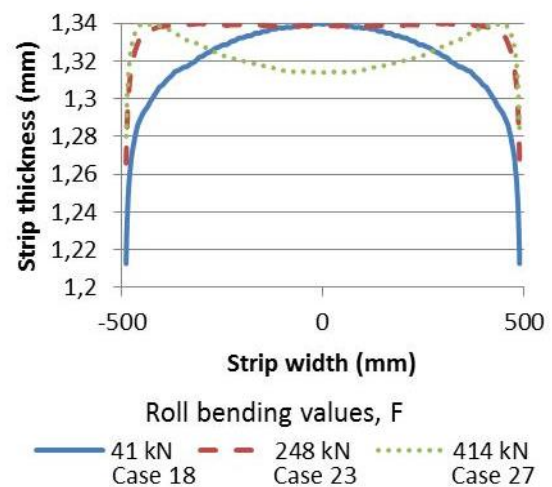


Figure 9. Exit strip thickness profile obtained with multiple roll bending force values

Table 5. Linear adjustment of the crown and edge drop in function of the modified parameters

Modified parameter	Strip crown (μm)		Strip edge drop (μm)	
	Equation of the linear adjustment	R^2	Equation of the linear adjustment	R^2
δ (mm)	$C = 0,424 * \delta + 19,7$	0,9944	$E_{40} = 0,0720 * \delta + 29,4$	0,8915
Work roll radius, R (mm)	$C = 0,164 * R + 4,82$	0,8049	$E_{40} = 0,146 * R + 1,07$	0,7219
Roll bending force, F (kN)	$C = -0,214 * F + 64,7$	0,9992	$E_{40} = -0,0372 * F + 37,2$	0,9851

Figures 10 and 11 present the normal contact pressures between the work and intermediate rolls, respectively caused by changing δ and roll bending force. Both are for the upper rolls. The first one shows that the peak changes in both magnitude and positioning. The second presents almost superimposed curves that differ only by its maximum values which were 1580 MPa, 1839 MPa and 2095 MPa for the respectively bending forces of 41 kN, 248 kN and 414 kN.

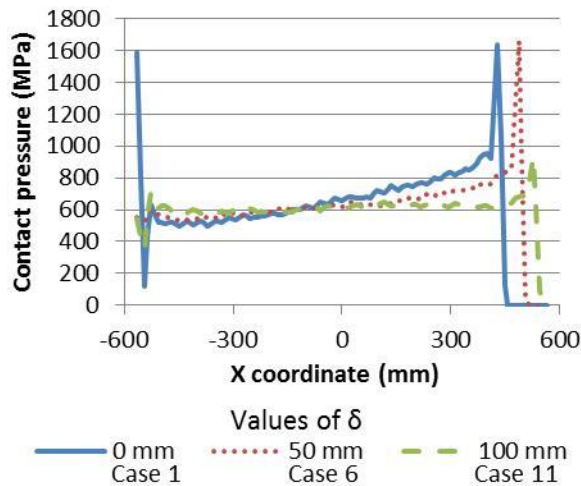


Figure 10. Contact normal pressures for multiple values of roll shift (δ)

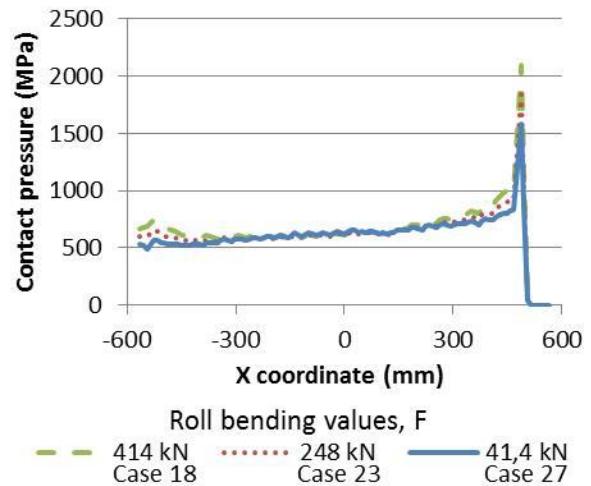


Figure 11. Contact normal pressures for multiple values of roll bending forces

2.4 Discussion

When compared to the other roll shift cases, δ and WR bending force of 108,6 kN was the one to yield the flattest strip. In this case, the right edge of the IMR as shown in Fig. 2 is exactly above the edge of the strip, which is consistent with the original idea (Kajiwara, *et al.*, 2015). However, the pressure presented in Fig. 10 shows that the contact only starts at position 448 mm, which means that the interaction was removed 42 mm beyond the unwanted portion on one side. This latter value corroborates with the results of Wang Q., *et al.* (2018) which are approximately 80 mm for a similar analysis.

Ginzburg and Azzam (1997) show that the work roll radius variation almost does not affect the strip profile when compared to the two other actuators considered in this analysis. For a range of 25 mm, the crown would change $-3 \mu\text{m}$, which is near the absolute value found in this paper, $5 \mu\text{m}$. It is probable that the signal difference is caused due to a different influence of this parameter on the equipment's vertical stiffness and total rolling force. This small variation of the strip's format may also justify the low correlation coefficients of the work roll radius modifications shown in Tab. 5. In this case, the small errors inherent to the utilized numerical model are nearly the same of the crown and edge drop range.

The oscillation near the length position -550 mm in Figs. 10 and 11 that doesn't have a high amplitude were also shown by Wang Q., *et al.* (2018). The remaining ones have a pressure peak among the highest values and are observed when δ is 0 mm, 40 mm and 80mm. They were probably caused by a sharp corner on the edge of the work roll barrel and by this region not being refined enough on the finite element model. The mesh should be remade for those three cases if they are used to define the maximum contact pressures between the WR and BUR. Since this exception does not occur in a place near the contact arc, it shouldn't affect the main results of strip quality.

3. CONCLUSION

This paper presents the correlations of the roll bending force, IMR shift δ and work roll radius to the strip's crown and edge drop. They can be used to better understand the rolling process and to achieve a better controlling strategy for the actuators. A reasonably linear function was found for IMR shifting and roll bending force, the influencing parameters, to the strip crown and edge drop.

The WR radius variation didn't impact very much on strip crown and edge drop very much, as was shown in Figs. 6 and 7, resulting in a 4 μm range for strip crown and 5 μm for edge drop, probably due to the inverse effect between lowering down both the rolling load and the roll flexibility on the strip crown.

Some of the results of contact pressures shown in Figs. 10 and 11 present inconsistencies that may be caused by a non-rounded geometry and a lack of more nodes at the edges of the rolls.

The 3D FEM/Multi-slab model was used in this sensitivity analysis and thanks to its high speed calculation, when compared to other full FE models, 27 cases could be processed in 2,5h on a relatively ordinary computer desktop.

This study has shown some preliminary results and more cases should be considered in order to yield more control rules for the 6-high rolling mill.

4. ACKNOWLEDGMENTS

The authors would like to thank CEFET-MG for funding the Masters scholarship of Renan Bueno Wojciechowski, a student at Mechanical Engineering Post-Graduate Program (PPGEM).

5. REFERENCES

- Aljabri, A., Jiang, Z.Y., Wei, D.B., Wang, X.D. and Tiba, H., 2013. "Thin Strip Profile Control Capability of Roll Crossing and Shifting in Cold Rolling Mill". *Materials Science Forum*, Vol. 773-774, p. 70-78.
- Ginzburg, V.B. and Azzam, M., 1997. "Selection of optimum strip profile and flatness technology for rolling mills". *Iron Steel Engineer*, Vol. 74, p. 30-38.
- Ginzburg, V.B. (editor), 2015. *Flat-rolled steel processes: advanced technologies*. CRC Press, Boca Raton.
- Kajiwara, T., Nishi, H., Yoshimura, Y. and Furumoto, H. *60 Excellent Inventions in Metal Forming*. Springer Berlin Heidelberg, Berlin.
- Linghu K., Jiang, Z., Zhao, J., Li, F., Wei, D., Xu, J., Zhang, X. and Zhao, X., 2014 "3D FEM analysis of strip shape during multi-pass rolling in a 6-high CVC cold rolling mill". *The International Journal of Advanced Manufacturing*, Vol. 74, p. 1733-1745.
- Shigaki Y., Wojciechowski, R.B. and Santos, S.C., 2019. "Recent improvements on the 3d Finite Element method/Multi-Slab method for flat rolling simulation". In *11th International Rolling Conference (IRC 2019)*. São Paulo, Brazil.
- Shigaki, Y., Montmitonnet, P. and Silva, J.M., 2017. "3D Finite Element Model for Roll Stack Deformation Coupled with a Multi-Slab Model for Strip Deformation for Flat Rolling Simulation". In *20th International ESAFORM Conference on Material Forming*. Dublin, Irlanda.
- Wang, Q.-L., Li, X., Hu, Y.-J., Sun, J. and Zhang, D.-H., 2018. "Numerical Analysis of Intermediate Roll Shifting-Induced Rigidity Characteristics of UCM Cold Rolling Mill". *Steel Research International*, Vol. 89, p. 1-13.
- Wang, Q.-L., Sun, J., Liu, Y.-M., Wang, P.-F. and Zhang, D.-H., 2017. "Analysis of symmetrical flatness actuator efficiencies for UCM cold rolling mill by 3D elastic-plastic FEM". *The International Journal of Advanced Manufacturing Technology*, Vol. 92, p. 1371-1389.
- Wang, X., Yang, Q., He, H., Sun, Y., Xu, D. and Liu, Y., 2020. "Effect of work roll shifting control on edge drop for 6-hi tandem cold mills based on finite element method model". *The International Journal of Advanced Manufacturing Technology*, Vol. 107, p. 2497-2511.

6. RESPONSIBILITY NOTICE

The authors are the only responsible for the printed material included in this paper.